

Efficient Combinatorial Optimization via Heat Diffusion

Hengyuan Ma¹, Wenlian Lu^{1,2,3,4,5,6}, Jianfeng Feng^{1,2,3,4,7*}

1 Institute of Science and Technology for Brain-inspired Intelligence, Fudan University, Shanghai 200433, China

2 Key Laboratory of Computational Neuroscience and Brain-Inspired Intelligence (Fudan University), Ministry of Education, China

3 School of Mathematical Sciences, Fudan University, No. 220 Handan Road, Shanghai, 200433, Shanghai, China

4 Shanghai Center for Mathematical Sciences, No. 220 Handan Road, Shanghai, 200433, Shanghai, China

5 Shanghai Key Laboratory for Contemporary Applied Mathematics, No. 220 Handan Road, Shanghai, 200433, Shanghai, China

6 Key Laboratory of Mathematics for Nonlinear Science, No. 220 Handan Road, Shanghai, 200433, Shanghai, China

7 Department of Computer Science, University of Warwick, Coventry, CV4 7AL, UK

* jffeng@fudan.edu.cn

ABSTRACT

Combinatorial optimization problems are widespread but inherently challenging due to their discrete nature. The primary limitation of existing methods is that they can only access a small fraction of the solution space at each iteration, resulting in limited efficiency for searching the global optimal. To overcome this challenge, diverging from conventional efforts of expanding the solver’s search scope, we focus on enabling information to actively propagate to the solver through heat diffusion. By transforming the target function while preserving its optima, heat diffusion facilitates information flow from distant regions to the solver, providing more efficient navigation. Utilizing heat diffusion, we propose a framework for solving general combinatorial optimization problems. The proposed methodology demonstrates superior performance across a range of the most challenging and widely encountered combinatorial optimizations. Echoing recent advancements in harnessing thermodynamics for generative artificial intelligence, our study further reveals its significant potential in advancing combinatorial optimization.

1 Introduction

Combinatorial optimization problems are prevalent in various applications, encompassing circuit design [1], machine learning [2], computer vision [3], molecular dynamics simulation [4], traffic flow optimization [5], and financial risk analysis [6]. This widespread application creates a significant demand for accelerated solutions to these problems. Alongside classical algorithms, which encompass both exact solvers and metaheuristics [7], recent years have seen remarkable advancements in addressing combinatorial optimization. These include quantum adiabatic approaches [8, 9, 10], simulated bifurcation [11, 12, 13], coherent Ising machine [14, 15], high-order Ising machine [16], and deep learning techniques [17, 18]. However, due to the exponential growth of the solution number, finding the optima within a limited computational budget remains a daunting challenge.

A key component of practical solutions for combinatorial optimization are the iterative approximation solvers. They typically begin with an initial solution and iteratively refine it by assessing potentially better solutions within the neighborhood of the current solution, known as the search scope or more vividly, *receptive field*. However, due to combinatorial explosion, as the scope of the receptive field increases, the number of solutions to be assessed grows exponentially, making a thorough evaluation of all these solutions computationally unfeasible. As a result, current approaches are limited to a narrow receptive field per iteration, rendering them blind to distant regions in the solution space and hence heightening the risk of getting trapped in local minimas or areas with bumpy landscapes. Although methods like large neighborhood search [19], variable neighborhood search [20] and path auxiliary sampling [21] are designed to broaden the search scope, they can only gather a modest increment of information from the expanded search scope. Consequently, the current solvers’ receptive field remains significantly constrained, impeding their search efficiency.

In this study, we approach the prevalent limitation from a unique perspective. Instead of expanding the solver’s receptive field to acquire more information from the solution space, we concentrate on propagating information from distant areas of the solution space to the solver via heat diffusion [22]. To illustrate, imagine a solver searching for the optima in the solution space akin to a person searching for a key in a dark room, as depicted in Fig. 1. Without light, the person is compelled to rely solely on touching his surrounding space. The tactile provides only localized information, leading to inefficient navigation. This mirrors the current situation in combinatorial optimization, wherein the receptive field is predominantly confined to local information. However, if the key were to emit heat, its radiating warmth would be perceptible from a distance, acting as a directional beacon. This would significantly enhance navigational efficiency for finding the key.

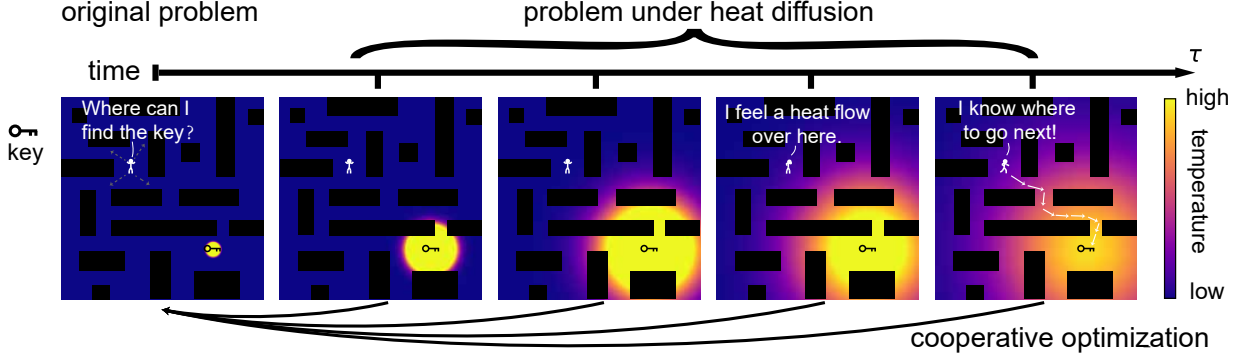


Figure 1: **The Heat diffusion optimization (HeO) framework.** The efficiency of searching a key in a dark room is significantly improved by employing navigation that utilizes heat emission from the key. In combinatorial optimization, heat diffusion transforms the target function into multiple versions, each directing information to the solver while preserving the original’s optimal solutions. These versions can be jointly optimized to solve the original problem..

Motivated by the above metaphor, we propose a simple but efficient framework utilizing heat diffusion to solve various combinatorial optimization problems. Heat diffusion transforms the target function into different versions, within which the information from distant regions actively flow toward the solver. Crucially, the backward uniqueness of the heat equation [23] guarantees that the original problem’s optima are unchanged under these transformations. Therefore, information of target functions under different heat diffusion transformations can be cooperatively employed for optimize the original problem (Fig. 1). Empirically, our framework demonstrates superior performance compared to advanced algorithms across a diverse range of combinatorial optimization instances, spanning quadratic to polynomial, binary to ternary, unconstrained to constrained, and discrete to mixed-variable scenarios. Mirroring the recent breakthroughs in generative artificial intelligence through diffusion processes [24], our research further reveals the potential of heat diffusion, a related thermodynamic phenomenon, in enhancing combinatorial optimization.

2 Gradient-based combinatorial optimization

Various combinatorial optimization problems can be naturally formalized as a pseudo-Boolean optimization (PBO) problem [25], in which we aim to find the minima of a real-value target function $f \in \mathbb{R}^n \mapsto \mathbb{R}$ subjecting to a binary constraints

$$\min_{\mathbf{s} \in \{-1, 1\}^n} f(\mathbf{s}), \quad (1)$$

where \mathbf{s} is binary configuration, and $f(\cdot)$ is the target function. Through the transformation $(\mathbf{s} + 1)/2$, our definition aligns with that in [26], where elements of \mathbf{s} take 0 or 1. Given the advanced development of gradient-based optimizers, we are interesting in converting discrete optimization problems into differentiable formats, thereby enabling gradient-based optimization methods. To achieve this purpose, we encode the bits $s_i, i = 1, \dots, n$ as independent Bernoulli variables $\text{Bern}(\theta_i)$ with $\theta_i \in [0, 1]$: $p(s_i = \pm 1 | \boldsymbol{\theta}) = 0.5 \pm (\theta_i - 0.5)$. In this way, the original combinatorial optimization problem is converted into a differentiable optimization problem

$$\min_{\boldsymbol{\theta} \in \mathcal{I}} h(\boldsymbol{\theta}), \quad (2)$$

where $\mathcal{I} := [0, 1]^n$, and $h(\boldsymbol{\theta}) = \mathbb{E}_{p(\mathbf{s}|\boldsymbol{\theta})}[f(\mathbf{s})]$. The minima $\boldsymbol{\theta}^*$ of Eq. (2) is $\boldsymbol{\theta}^* = 0.5(\text{sgn}(\mathbf{s}^*) + 1)$, given that \mathbf{s}^* is a minima of the original problem Eq. (1), here $\text{sgn}(\cdot)$ is the sign function. Now Eq. (2) can be solved through gradient descent starting from some $\boldsymbol{\theta}_0$

$$\boldsymbol{\theta}_{t+1} = \boldsymbol{\theta}_t - \gamma \nabla_{\boldsymbol{\theta}_t} h(\boldsymbol{\theta}_t), \quad (3)$$

for $t = 1, \dots, T$, given the learning rate γ and minimum iteration number T .

2.1 Parameter uncertainty

A primary concern arises as the optimization procedure Eq. (3) gives a distribution $p(\mathbf{s}|\boldsymbol{\theta})$ over the whole configuration space $\{-1, 1\}^n$ instead of a deterministic binary configuration \mathbf{s} . The uncertainty of $p(\mathbf{s}|\boldsymbol{\theta})$, which is measured by its

total variance

$$V(\boldsymbol{\theta}) = \sum_{i=1}^n \theta_i(1 - \theta_i), \quad (4)$$

makes it still ambiguous which binary configuration is the best one. Although we can manually binarize $\boldsymbol{\theta}$ through $\mathbf{B}(\boldsymbol{\theta}) := \text{sgn}(\boldsymbol{\theta} - 0.5)$ to get the binary configuration which maximizes probability $p(\mathbf{s}|\boldsymbol{\theta})$, the outcome $f(\mathbf{B}(\boldsymbol{\theta}))$ may be much higher than $h(\boldsymbol{\theta})$, resulting in significant performance degradation [27]. This suggests that a good gradient-based algorithm should efficiently reduce the uncertainty $V(\boldsymbol{\theta})$ to zero after optimization.

2.2 Monte Carlo gradient estimation

Conventionally, we can solve the problem Eq. (2) by approximating the gradient of $h(\boldsymbol{\theta})$ via Monte Carlo gradient estimation (MCGE) [28], in which we estimate the gradient in Eq. (3) as

$$\begin{aligned} \nabla_{\boldsymbol{\theta}} h(\boldsymbol{\theta}) &= \nabla_{\boldsymbol{\theta}} \mathbb{E}_{p(\mathbf{s}|\boldsymbol{\theta})}[f(\mathbf{s})] = \mathbb{E}_{p(\mathbf{s}|\boldsymbol{\theta})}[f(\mathbf{s}) \nabla_{\boldsymbol{\theta}} \log p(\mathbf{s}|\boldsymbol{\theta})] \\ &\approx \frac{1}{M} \sum_{m=1}^M f(\mathbf{s}^{(m)}) \nabla_{\boldsymbol{\theta}} \log p(\mathbf{s}^{(m)}|\boldsymbol{\theta}), \quad \mathbf{s}^{(m)} \sim_{i.i.d.} p(\mathbf{s}|\boldsymbol{\theta}), \quad m = 1, \dots, M, \end{aligned} \quad (5)$$

as shown in Alg. 1. Noticed that we clamp the parameter $\boldsymbol{\theta}_t$ in the $[0, 1]$ for numerical stability; additionally, we binarize the $\boldsymbol{\theta}_T$ to obtain the optimized binary configuration \mathbf{s}_T in the end.

Algorithm 1 Monte Carlo gradient estimation for combinatorial optimization (MCGE)

Input: target function $f(\cdot)$, step size γ , sample number M , iteration number T
 initialize elements of $\boldsymbol{\theta}_0$ as 0.5
for $t = 0$ **to** $T - 1$ **do**
 sample $\mathbf{s}^{(m)} \sim_{i.i.d.} p(\mathbf{s}|\boldsymbol{\theta}_t), \quad m = 1, \dots, M$
 $\mathbf{g}_t \leftarrow \frac{1}{M} \sum_{m=1}^M f(\mathbf{s}^{(m)}) \nabla_{\boldsymbol{\theta}_t} \log p(\mathbf{s}^{(m)}|\boldsymbol{\theta}_t)$
 $\boldsymbol{\theta}_{t+1} \leftarrow \text{clamp}(\boldsymbol{\theta}_t - \gamma \mathbf{g}_t, 0, 1)$
end for
 $\mathbf{s}_T \leftarrow \text{sgn}(\boldsymbol{\theta}_T - 0.5)$
Output: binary configuration \mathbf{s}_T

It turns out that the MCGE (Alg. 1) performs poorly compared to existing solvers such as simulated annealing and Hopfield neural network, as shown in Fig. 2. We explain this inferior performance of MCGE as follows. Although MCGE turns the combinatorial optimization problem into a differentiable one, it does not reduce the inherent complexity of the original problem, and the challenge shifts to navigating the complex energy landscape. This issue is not ameliorated even when applying advanced gradient-based solver such as momentum method. As gradient only provides local information, MCGE might be easily ensnared in local minima. We also find that the MCGE are struggling to minimize the uncertainty $V(\boldsymbol{\theta})$, as shown in Fig. 2. This observation clarifies why, notwithstanding the widespread use of MCGE in machine learning, there seems to be an absence, to the best of our knowledge, of studies that directly employ MCGE specifically for combinatorial optimization.

3 Heat diffusion optimization

The suboptimal performance of the MCGE can be attributed to its reliance on a narrow receptive field at each iteration, a limitation shared with other existing methods. We manage to provide more efficient navigation to the gradient-based solver by employing heat diffusion, which propagates information from distant region to the solver. Intuitively, we consider the parameter space as a thermodynamic system, where each parameter θ is referred to as a location and is associated with an initial temperature value $h(\boldsymbol{\theta})$, as shown in Fig. 1. Then optimization procedure can be described as the process that the solver is walking around the parameter space to search for the location $\boldsymbol{\theta}^*$ with the highest temperature (equivalently, the lowest $h(\boldsymbol{\theta})$). As time progresses, heat flows obeying the principles of heat transfer, leading to a dynamic temperature distribution at various moments. The heat at the maxima $\boldsymbol{\theta}^*$ flows to other regions, reaching the location of the solver. This heat flow conveys useful information for the solver to find the maxima, as the solver can follow the direction that heat come from to get to the maxima.

Now we introduce heat diffusion for solving the combinatorial optimization. We extend the parameter space of $\boldsymbol{\theta}$ from $[0, 1]^n$ to $\bar{\mathbb{R}}^n$ with $\bar{\mathbb{R}} = \mathbb{R} \cup \{-\infty, +\infty\}$. To keep the probabilistic distribution $p(\mathbf{s}|\boldsymbol{\theta})$ meaningful for

$\theta \notin [0, 1]^n$, we now define $p(s_i = \pm 1 | \theta) = \text{clamp}(0.5 \pm (\theta_i - 0.5), 0, 1)$, where the clamp function is defined as $\text{clamp}(x, 0, 1) = \max(0, \min(x, 1))$. Due to heat exchange between locations at the parameter space, the temperature distribution $h(\theta)$ varies across time τ . Denote the temperature distribution at τ as $u(\tau, \theta)$, then $u(\tau, \theta)$ is the solution to the following unbounded heat diffusion equation

$$\begin{cases} \partial_\tau u(\tau, \theta) &= \Delta_\theta u(\tau, \theta), & \tau > 0, & \theta \in \mathbb{R}^n \\ u(\tau, \theta) &= h(\theta), & \tau = 0, & \theta \in \mathbb{R}^n. \end{cases} \quad (6)$$

For $\theta \in \bar{\mathbb{R}}^n / \mathbb{R}^n$, we complement the definition by $u(\tau, \theta) = \lim_{\theta_n \rightarrow \theta} u(\tau, \theta_n)$, where $\{\theta_n\}$ is a sequence in \mathbb{R}^n with limitation θ . The heat diffusion equation exhibits two crucial characteristics that facilitate its application in efficient optimization. Firstly, the propagation speed of heat is infinite [22], implying that information carried by heat from distant locations reaches the solver instantaneously. Secondly, heat always spontaneously flows from areas of higher temperature to lower temperature. This suggests that the location of each local maxima (including the global maxima) does not change across time τ . In fact, we have the following theorem.

Theorem 1. *For any $\tau > 0$, the function $u(\tau, \theta)$ and $h(\theta)$ has the same global maxima in $\bar{\mathbb{R}}^n$*

$$\arg \max_{\theta \in \bar{\mathbb{R}}^n} u(\tau, \theta) = \arg \max_{\theta \in \bar{\mathbb{R}}^n} h(\theta) \quad (7)$$

Consequently, we can generalize the gradient descent approach Eq. (3) by substituting the function $h(\theta)$ with $u(\tau, \theta)$ with different $\tau > 0$ at different steps, as follows

$$\theta_{t+1} = \theta_t - \gamma \nabla_{\theta_t} u(\tau_t, \theta_t), \quad (8)$$

where the subscript ' t ' in τ_t means that τ_t can vary across different steps. In this way, the optimizer receives the gradients containing information about distant region of the landscape that is propagated by the heat diffusion, resulting in a more efficient navigation. However, the iteration of Eq. (8) will converge to $\check{\theta}$ which is defined as

$$\check{\theta}_i = \begin{cases} +\infty, & s_i^* = +1 \\ -\infty, & s_i^* = -1 \end{cases}. \quad (9)$$

Noticed that projecting the $\check{\theta}$ back to \mathcal{I} gives the maxima of $h(\theta)$ in \mathcal{I} : $\theta^* = \text{Proj}_{\mathcal{I}}(\check{\theta})$. To make the optimization process Eq. (8) practicable, we project the θ_t back to \mathcal{I} after gradient descent at each iteration

$$\theta_{t+1} = \text{Proj}_{\mathcal{I}}(\theta_t - \gamma \nabla_{\theta_t} u(\tau_t, \theta_t)), \quad (10)$$

so that $\theta_t \in \mathcal{I}$ always holds. Importantly, due to the property of the projection, if the solver moves along the towards $\check{\theta}$, it also gets closer to θ^* . Therefore, Eq. (10) is a reasonable update rule for finding the maxima θ^* within in \mathcal{I} . Additionally, since the convergence of Eq. (8) is $\check{\theta}$, whose coordination are all infinity, the convergent point of Eq. (10) must within the vertices of \mathcal{I} , i.e., $\{0, 1\}^n$. This suggests that Eq. 10 is guaranteed to give an output θ diminishing the uncertainty $V(\theta)$.

3.1 Heat equation estimation

Motivated by the above theoretical analysis, we now develop an efficient algorithm for solving the combinatorial optimization problem. The first issue is to solve the heat diffusion equation Eq. (6) given the target function $f(\cdot)$. When the dimension n is high, this is computational expensive in general. The solution of Eq. (6) can be written in a form which has a obviously probabilistic meaning

$$u(\tau, \theta) = \mathbb{E}_{p(\mathbf{z})}[h(\theta + \sqrt{2\tau}\mathbf{z})], \quad p(\mathbf{z}) = \mathcal{N}(\mathbf{0}, I). \quad (11)$$

Combined with the definition of $h(\theta)$, we have

$$u(\tau, \theta) = \mathbb{E}_{p(\mathbf{z})}[\mathbb{E}_{p(\mathbf{s}|\theta + \sqrt{2\tau}\mathbf{z})}[f(\mathbf{s})]]. \quad (12)$$

To construct a low-variance estimation, instead of directly using the Monte Carlo gradient estimation by sampling from $p(\mathbf{z})$ and $p(\mathbf{s}|\theta + \sqrt{2\tau}\mathbf{z})$ for gradient estimation, we manage to integrate out the stochasticity respect to \mathbf{z} . We reparameterize the $p(\mathbf{s}|\theta)$ by introducing another random vector $\mathbf{x} \in \mathbb{R}^n$, which is uniformly distributed on $(0, 1)^n$. It is easy to see that $\text{sgn}(\theta_i - x_i) \sim \text{Bern}(\theta_i)$. Replacing s_i by x_i in Eq. (2), we have a new expression of $h(\theta)$

$$h(\theta) = \mathbb{E}_{p(\mathbf{x})}[f(\text{sgn}(\theta - \mathbf{x}))], \quad \mathbf{x} \sim \text{Unif}(0, 1)^n, \quad (13)$$

where $\text{sgn}(\cdot)$ is element-wise sign function. Combine Eq. (11) and Eq. (13) and exchange the order of integration, we have

$$u(\tau, \theta) = \mathbb{E}_{p(\mathbf{x})}[\mathbb{E}_{p(\mathbf{z})}[f(\text{sgn}(\theta + \sqrt{2\tau}\mathbf{z} - \mathbf{x}))]]. \quad (14)$$

Now we calculate the inner term $\mathbb{E}_{p(\mathbf{z})}[f(\text{sgn}(\boldsymbol{\theta} + \sqrt{2\tau}\mathbf{z} - \mathbf{x}))]$. Assume the target function $f(\mathbf{s})$ can be written as a K -order multilinear polynomial of \mathbf{s}

$$f(\mathbf{s}) = a_0 + \sum_{i_1} a_{1,i_1} s_{i_1} + \sum_{i_1 < i_2} a_{2,i_1 i_2} s_{i_1} s_{i_2} + \sum_{i_1 < i_2 < i_3} a_{3,i_1 i_2 i_3} s_{i_1} s_{i_2} s_{i_3} + \cdots + \sum_{i_1 < \cdots < i_K} a_{K,i_1 \dots i_K} s_{i_1} \cdots s_{i_K}, \quad (15)$$

which is the case that for a wide range of combinatorial optimization problems [16]. We have

$$\mathbb{E}_{p(\mathbf{z})}[f(\text{sgn}(\boldsymbol{\theta} + \sqrt{2\tau}\mathbf{z} - \mathbf{x}))] \quad (16)$$

$$= a_0 + \sum_{i_1} a_{1,i_1} \tilde{s}_{i_1} + \sum_{i_1 < i_2} a_{2,i_1 i_2} \tilde{s}_{i_1} \tilde{s}_{i_2} + \sum_{i_1 < i_2 < i_3} a_{3,i_1 i_2 i_3} \tilde{s}_{i_1} \tilde{s}_{i_2} \tilde{s}_{i_3} + \cdots + \sum_{i_1 < \cdots < i_K} a_{K,i_1 \dots i_K} \tilde{s}_{i_1} \cdots \tilde{s}_{i_K}, \quad (17)$$

where

$$\tilde{s}_i = \mathbb{E}_{p(z_i)}[\text{sgn}(\theta_i + \sqrt{2\tau}z_i - x_i)] = \text{erf}\left(\frac{\theta_i - x_i}{\sqrt{2\tau}}\right), \quad (18)$$

where $\text{erf}(\cdot)$ is the error function. Therefore, we have

$$u(\tau, \boldsymbol{\theta}) = \mathbb{E}_{p(\mathbf{x})}[f(\text{erf}(\frac{\boldsymbol{\theta} - \mathbf{x}}{\sqrt{2\tau}}))], \quad (19)$$

where $\text{erf}(\cdot)$ is the element-wise error function. For the case that the target function $f(\mathbf{s})$ is not a multilinear polynomial of \mathbf{s} , we still use the approximation Eq. (19), as we empirically find that the approximation works well.

3.2 Proposed algorithm

Basde on Eq. (19), we estimate the gradient of $u(\tau, \boldsymbol{\theta})$ as

$$\nabla_{\boldsymbol{\theta}} u(\tau, \boldsymbol{\theta}) \approx \frac{1}{M} \sum_{m=1}^M \nabla_{\boldsymbol{\theta}} f(\text{erf}(\frac{\boldsymbol{\theta} - \mathbf{x}^{(m)}}{\sqrt{2\tau}})), \quad \mathbf{x}^{(m)} \sim_{i.i.d.} \text{Unif}[0, 1]^n. \quad (20)$$

This can be accelerated by GPUs, making the framework scalable for high-dimensional cases. We illustrate the algorithm for combinatorial optimization in Alg. 2, which we call *Heat diffusion optimization (HeO)*, where we set the sample number M as 1. Our HeO can be equipped with momentum, which is shown in Alg. 3 in *Appendix*. In contrast to those methods specially designed for solving combinatorial optimization with special form such as quadratic unconstrained binary optimization which only involve 2-order interactions between individual bits s_i , our HeO can directly solve PBO problems with general form. Although PBO can be represented as QUBO [29], this necessitates the introduction of auxiliary variables, which may consequently increase the problem size and leading to additional computational overhead. In fact, there exist some PBO that require at least $O(2^{n/2})$ auxiliary variables to reformulate them into QUBO [30], making it unfeasible for solving in these ways.

Algorithm 2 Heat diffusion optimization (HeO)

Input: target function $f(\cdot)$, step size γ , τ schedule $\{\tau_t\}$, iteration number T
initialize elements of $\boldsymbol{\theta}_0$ as 0.5
for $t = 0$ **to** $T - 1$ **do**
 sample $\mathbf{x}_t \sim \text{Unif}[0, 1]^n$
 $\mathbf{g}_t \leftarrow \nabla_{\boldsymbol{\theta}_t} f(\text{erf}(\frac{\boldsymbol{\theta}_t - \mathbf{x}_t}{\sqrt{2\tau_t}}))$
 $\boldsymbol{\theta}_{t+1} \leftarrow \text{Proj}_{\mathcal{I}}(\boldsymbol{\theta}_t - \gamma \mathbf{g}_t)$
end for
 $\mathbf{s}_T \leftarrow \text{sgn}(\boldsymbol{\theta}_T - 0.5)$
Output: binary configuration \mathbf{s}_T

3.3 Error bound analysis

One counter-intuitive thing is that due to Eq. (10), the HeO actually are optimize $u(\tau_t, \boldsymbol{\theta})$ at each step t , as the solver moves along the gradient $\nabla_{\boldsymbol{\theta}} u(\tau_t, \boldsymbol{\theta})$. It seems weird that we are optimizing $h(\boldsymbol{\theta})$ by concurrently optimizing different functions $u(\tau_t, \boldsymbol{\theta})$. Actually, the optimization of different $u(\tau, \boldsymbol{\theta})$ coordinately help to the optimization of $h(\boldsymbol{\theta})$. We illustrate this by provide a theoretical upper bound for the optimization loss $h(\boldsymbol{\theta}) - h(\boldsymbol{\theta}^*)$ related to $u(\tau, \boldsymbol{\theta}) - u(\tau, \boldsymbol{\theta}^*)$, the optimization loss for $u(\tau, \boldsymbol{\theta})$, $\tau > 0$.

Theorem 2. Given $\tau_2 > 0$ and $\epsilon > 0$, there exists $\tau_1 \in (0, \tau_2)$, such that

$$h(\theta^*) - h(\theta) \leq (f^* - f_{\min})^{1/2} \left[(u(\tau_2, \theta^*) - u(\tau_2, \theta) + \frac{n}{2} \int_{\tau_1}^{\tau_2} \frac{u(\tau, \theta^*) - u(\tau, \theta)}{\tau} d\tau)^{1/2} + \epsilon \right]. \quad (21)$$

Consequently, we can simultaneously optimize a series σ -diffusion problem to solve the original PBO problem, which we refer to as a *cooperative optimization* paradigm, as illustrated in Fig. 1.

4 Experiments

We apply our HeO on several challenging combinatorial optimization problems. Unless explicitly stated otherwise, we employ the τ_t schedule as $\sqrt{2\tau_t} = 1 - t/T$ for Alg. 2 throughout this work. This choice is motivated by the aim to reverse the direction of heat flow back, guiding the solver towards the origin of the source, i.e., the global minima. Noticed that this choice is not theoretically necessary, as elaborated in *Discussion*.

4.1 Toy example

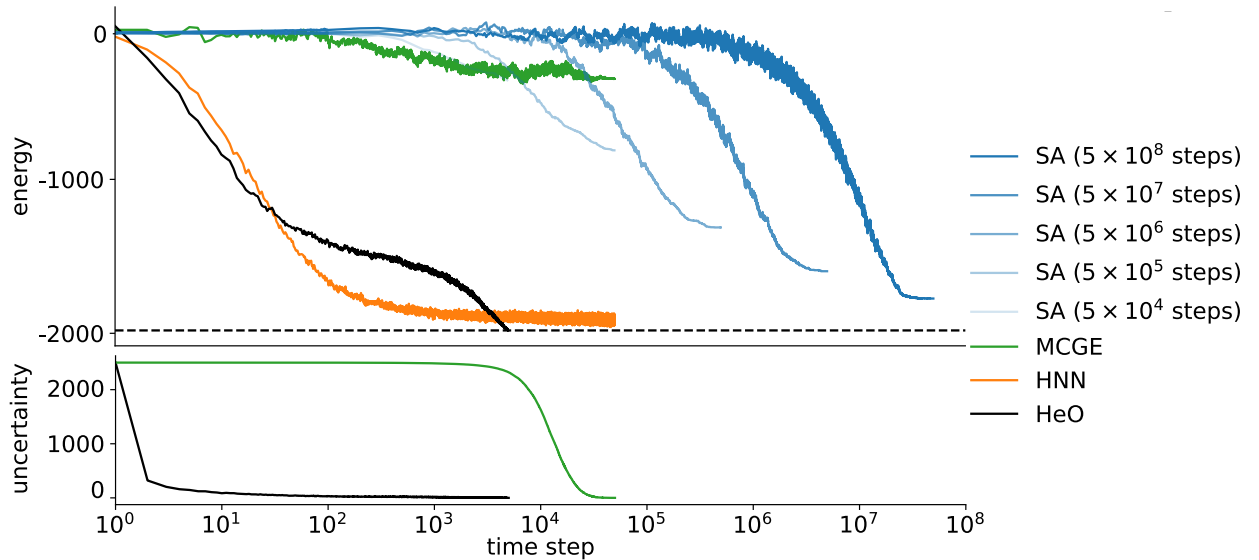


Figure 2: Performance of HeO, Monte Carlo gradient estimation (MCGE), Hopfield neural network (HNN) and simulated annealing (SA) with different time steps on the nonlinear binary optimization problem (Eq. (22)). Top panel: the energy (target function $f(\cdot)$). Bottom panel: the uncertainty $V(\theta)$ (Eq. (4)) of HeO and MCGE.

To illustrate the efficacy of our HeO for handling general combinatorial optimization problem, we compare the performance of our HeO against several representative methods: the conventional probabilistic parameterization solver MCGE [28], the simulated annealing [31], and the Hopfield neural network [32]. We consider the following randomly constructed neural network target function

$$f(\mathbf{s}) = \mathbf{a}_2^T \text{sigmoid}(W\mathbf{s} + \mathbf{a}_1) \quad (22)$$

where $\text{sigmoid}(x) = \frac{1}{1+e^{-x}}$ is the element-wise sigmoid function, $\mathbf{a}_1 \in \mathbb{R}^n$, $\mathbf{a}_2 \in \mathbb{R}^m$, $W \in \mathbb{R}^{m,n}$ are randomly sampled network parameters. The elements of \mathbf{a}_1 , \mathbf{a}_2 , W and uniformly sampled from $[-1, 1]$. According to the universal approximation theory [33], $f(\mathbf{s})$ can approximate any measurable function with sufficiently large m and n , thereby representing a general PBO. We apply HeO with momentum (Alg. 3). As shown in Fig. 2, where we set $n, m = 10000$, our HeO demonstrates exceptional superiority over all other methods, and efficiently reduces its uncertainty compared to MCGE.

We apply our HeO to a variety of combinatorial optimization problems, including QUBO, polynomial unconstrained binary optimization (PUBO), ternary optimization, mixed combinatorial optimization, and constrained binary optimization, demonstrating its versatility and broad applicability.

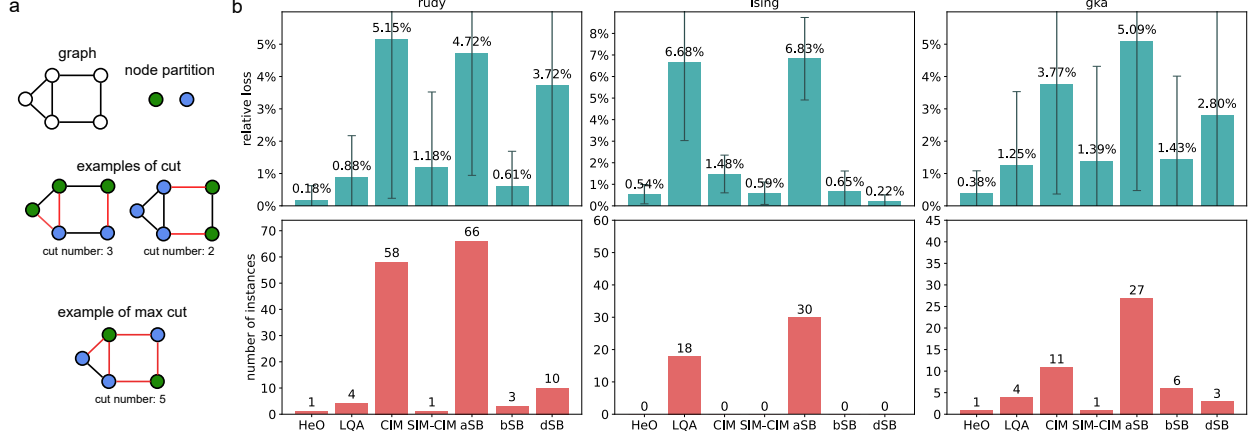


Figure 3: a, Illustration of the max-cut problem. b, Performance of HeO and representative approaches including LQA [10], aSB [12], bSB [13], dSB [13], CIM [34] and SIM-CIM [15] on Max-cut problems from the Biq Mac Library [35]. Top panel: average relative loss for each algorithm over all problems. Bottom panel: the count of instances where each algorithm ended up with one of the bottom-2 worst results among the 7 algorithms.

4.2 Quadratic unconstrained binary optimization

The QUBO is the combinatorial optimization problem with quadratic form target function

$$f(\mathbf{s}) = \mathbf{s}^T J \mathbf{s}, \quad (23)$$

where $J \in \mathbb{R}^{n \times n}$ is a symmetric matrix with zero diagonals. A well-known class of QUBO is max-cut problem [27], which involves dividing the vertices of a graph into two distinct subsets in such a way that the number of edges between the two subsets is maximized. The max-cut problem is NP-hard, and can be equivalently formulated as the quadratic form Eq. (23), where J is determined by the adjacency matrix of the graph, and maximizing the cut-value is equivalent to minimize $f(\mathbf{s})$.

We compare our HeO with representative methods especially developed for solving QUBO including LQA [10], aSB [12], bSB [13], dSB [13], CIM [34], and SIM-CIM [15] on the 3 sets of max-cut problems in the Biq Mac Library [35]¹. To reduce the fluctuations of the results, for each algorithm alg and instant i , the relative loss is calculated as $|C_{\min}^{i, \text{alg}} - C_{\min}^i| / |C_{\min}^i|$, where $C_{\min}^{i, \text{alg}}$ is the lowest output of the algorithm alg on the instance i over 10 tries, and C_{\min}^i is the lowest output of all 7 the algorithm on the instance i . We report the relative loss averaged over all instances and the count of the instances where each algorithm ended up with one of the bottom-2 worse results among the 7 algorithms in Fig. 3. It is observed that our HeO is superior to other methods in terms of the relative loss, and stands out as the only one that consistently avoids producing the bottom-2 worst results. This performance emphasizes our HeO's significant potential in handling QUBO, a critical category of combinatorial optimization.

4.3 Polynomial unconstrained binary optimization

PUBO is a class of combinatorial optimization problems, in which higher-order interactions between bits s_i appears in the target function. Existing methods for solving PUBO fall into two categories: the first approach involves transforming PUBO into QUBO by adding auxiliary variables through a quadratization process, and then solving it as a QUBO problem [37], and the one directly solves PUBO [16]. The quadratization process may dramatically increases the dimension of the problem, hence brings heavier computational overhead. On the contrary, our HeO can be directly used for solving PUBO.

A well-known class of PUBO is the Boolean 3-satisfiability (3-SAT) problem [27], which is NP-complete. The 3-SAT problem involves determining the satisfiability of a Boolean formula over n Boolean variables b_1, \dots, b_n where $b_i \in \{0, 1\}$. The Boolean formula is structured in Conjunctive Normal Form (CNF) consisting of H conjunction (\wedge) of clauses, and each clause h is a disjunction (\vee) of exactly three literals. A literal is either a Boolean variable or its negation. An algorithm of 3-SAT aims to find the Boolean variables that makes as many as clauses satisfied.

¹<https://biqmac.aau.at/biqmaclib.html>

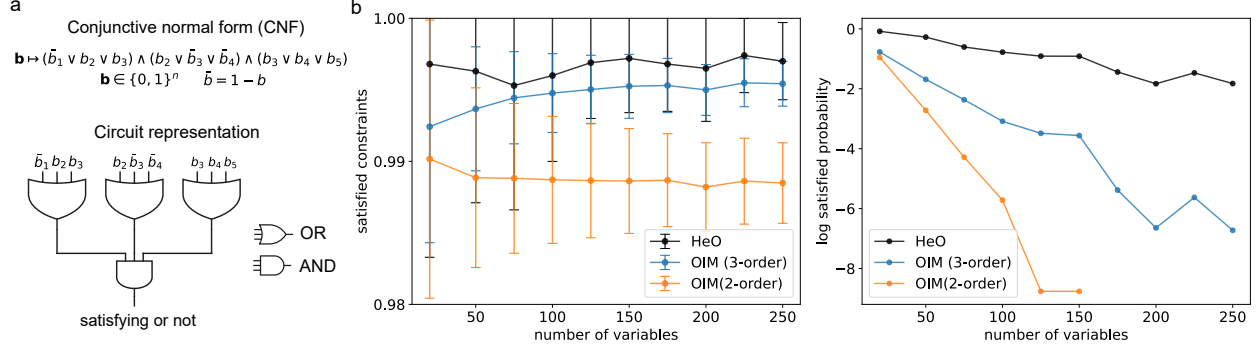


Figure 4: a, Illustration of the Boolean 3-satisfiability (3-SAT) problem. b, The 3-SAT problems with various number of variables from the SATLIB [36]. Top panel: The mean percent of constraints satisfied of HeO, 2-order and 3-order oscillator Ising machine (OIM) [16] under various numbers of the variables in the 3-SAT. Bottom panel: The probability of satisfying all constraints of each algorithm versus the number of the variables in the 3-SAT problems.

To apply our HeO to the 3-SAT, we formulate 3-SAT as a PBO. We encode each Boolean variable b_i as s_i , which is assigned with value 1 if $b_i = 1$, otherwise $s_i = -1$. For a literal, we define a value c_{h_i} , which is -1 if the literal is the negation of the corresponding Boolean variable, otherwise it is 1. Then finding the Boolean variables that makes as many as clauses satisfied is equivalent to minimize the target function

$$f(\mathbf{s}) = \sum_{h=1}^H \prod_{i=1}^3 \frac{1 - c_{h_i} s_{h_i}}{2}. \quad (24)$$

We compared our HeO with the second-order oscillator Ising machines (OIM) solver that using quadratization and the state-of-art high-order OIM proposed in [16] on 3-SAT instance in SATLIB². As shown in Fig. 4, our HeO is superior to other methods in attaining higher number of satisfied solutions. Notably, our method is able to find satisfiable solutions to the 250-variable 3-SAT problems, which is just achieved by the higher-order oscillator Ising machine recently, while the 2-order oscillator Ising machines have been unable to find solutions satisfying all clauses before [16]. This highlights our HeO significant potential in handling higher-order combinatorial optimization problems.

4.4 Ternary optimization

Neural networks excel in learning and modeling complex functions. However, neural networks comprising a vast number of parameters can bring about considerable computational demands. A promising strategy to mitigate this issue involves constraining parameters to discrete values, significantly reducing memory usage during inference and enhancing implementation efficiency [38]. Among such efforts is the adoption of ternary value parameters $(-1, 0, 1)$, which simplifies computations by eliminating the need for multipliers. Yet, training networks with discrete parameters introduces a significant challenge due to the high-dimensional combinatorial optimization problem it presents.

We apply our HeO to train neural networks with ternary value. Supposed that we have an input-output dataset \mathcal{D} generated by a ground-truth ternary single-layer perceptron $\Gamma(\mathbf{v}; W_{\text{GT}}) = \text{Relu}(W_{\text{GT}}\mathbf{v})$, where $\text{Relu}(x) = \max\{0, x\}$ is the element-wise Relu activation, $W_{\text{GT}} \in \{-1, 0, 1\}^{m \times n}$ is the ground-truth ternary weight parameter, $\mathbf{v} \in \{-1, 0, 1\}^n$ is the input. We aim to find the ternary configuration $W \in \{-1, 0, 1\}^{m \times n}$ minimizing the MSE

$$\text{MSE}(W, \mathcal{D}) = \frac{1}{|\mathcal{D}|} \sum_{(\mathbf{v}, \mathbf{y}) \in \mathcal{D}} \|\Gamma(\mathbf{v}; W) - \mathbf{y}\|^2. \quad (25)$$

where $\mathbf{y} = \Gamma(\mathbf{v}; W_{\text{GT}}) \in \mathbb{R}^m$ is the model output.

We generalized our HeO from the binary to the ternary case by representing a ternary variable $s_t \in \{-1, 0, 1\}$ as $s_t = \frac{1}{2}(s_{b,1} + s_{b,2})$ with two bits $s_{b,1}, s_{b,2} \in \{-1, 1\}$. In this way, each element of W can be represented as a function of $\mathbf{s} \in \mathbb{R}^{m \times n \times 2}$. We denote this relation as a matrix-value function $W = W(\mathbf{s})$

$$W_{ij}(\mathbf{s}) = \frac{1}{2}(s_{ij,1} + s_{ij,2}), \quad i = 1, \dots, m, \quad j = 1, \dots, n, \quad (26)$$

²<https://www.cs.ubc.ca/~hoos/SATLIB/benchm.html>

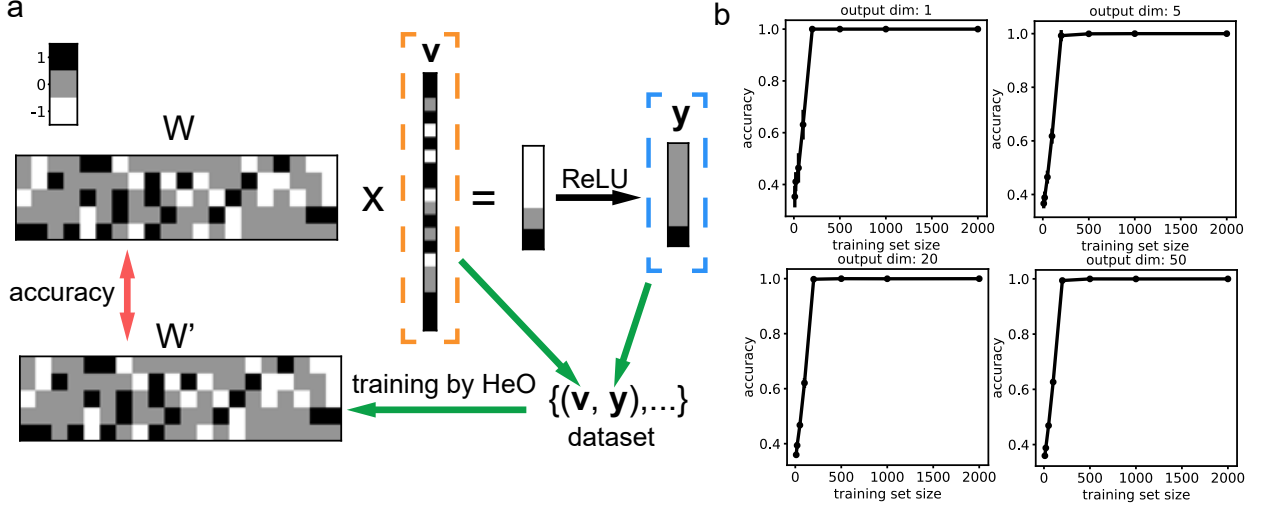


Figure 5: a, Training a network with ternary-value $(-1, 0, 1)$ weight based on input-output pairs. b, The weight value accuracy of the HeO under different sizes of training set. ($n = 100, m = 1, 5, 20, 50$). For each test, we estimate the mean from 10 runs, and the standard deviation is small hence imperceptible.

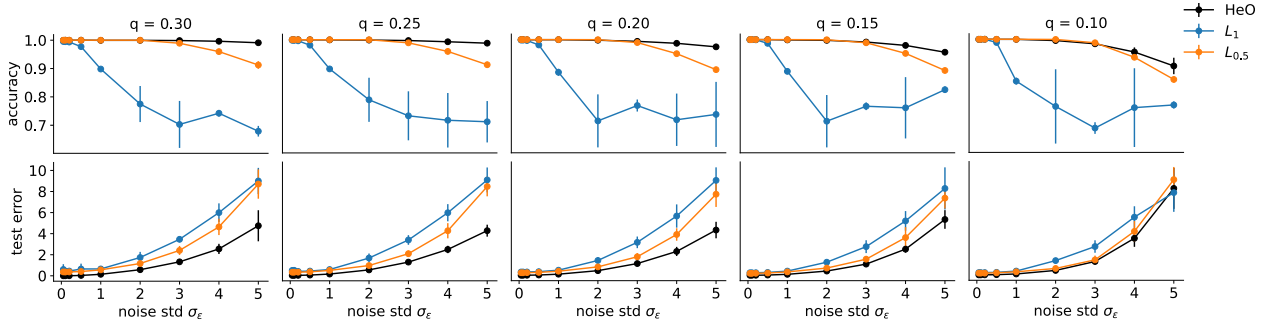


Figure 6: The variable selection of 400-dimensional linear regressions using HeO and Lasso (L_1) regression [39] and $L_{0.5}$ regression [40]. We consider the cases of $q = 0.05, 0.1$ and report the accuracy of each algorithm in determining whether each variable should be ignored for prediction and their MSE on the test set. The mean (dots) and standard deviation (bars) are estimated over 10 runs.

and the target function is defined as

$$f(\mathbf{s}) = \frac{1}{|\mathcal{D}|} \sum_{(\mathbf{v}, \mathbf{y}) \in \mathcal{D}} \|\Gamma(\mathbf{v}; W(\mathbf{s})) - \mathbf{y}\|^2. \quad (27)$$

As shown in Fig. 5, with the increasing in $|\mathcal{D}|$, the accuracy of the learned weight values quickly increases to 1. This highlights the potential of our HeO in learning intricate discrete structures under different output size $m = 1, 5, 20, 50$. Noticed that the lower the output dimension m and training set size are, the harder the task is.

4.5 Mixed combinatorial optimization

In high-dimensional linear regression, the presence of numerous variables, among which only a small fraction significantly contribute to prediction, is a common scenario. Therefore, identifying and selecting a subset of variables with strong predictive power—a process known as variable selection—is crucial. This practice not only improves the model's generalizability and computational efficiency but also enhances its interpretability. [41]. However, direct variable selection is a combinatorial optimization mixed with continuous variables, entailing tackling NP-hard problems [42]. As a practical alternative, regularization methods like lasso algorithm are commonly employed [39].

Consider a dataset generated from a linear model, in which the input \mathbf{v} obeys a standard Gaussian distribution, and the output is generated by $y = \beta^* \cdot \mathbf{v} + \epsilon$, where β^* is the ground-truth linear coefficient and ϵ is independent Gaussian noise with standard deviation σ_ϵ . Suppose that a substantial proportion of its elements β_i^* are zero, hence only a small proportion (denoted as $q \in (0, 1)$) of variables should be considered for prediction. Our goal is to identify these variables through an indicator vector $\mathbf{s} \in \{-1, 1\}^n$ (where 1 indicates selection and -1 indicates non-selection) and estimate the coefficient β . The target function of the problem can be written as

$$f(\mathbf{s}; \beta) = \frac{1}{|\mathcal{D}|} \sum_{(\mathbf{v}, \mathbf{y}) \in \mathcal{D}} \left| \left(\beta \odot \frac{\mathbf{s} + \mathbf{1}}{2} \right) \cdot \mathbf{v} - \mathbf{y} \right|^2, \quad (28)$$

where $\mathbf{1} \in \mathbb{R}^n$ is the vector whose elements are all 1.

We develop an algorithm based on HeO for this mixed combinatorial optimization (Alg. 5, *Appendix*). We parameterize the distribution of \mathbf{s} as θ as before, and minimize the fitting loss relative to θ while slowly changing β via its error gradient. After binarizing the resulting θ to get the indicator \mathbf{s} , we implement an ordinary least squares regression on the variables selected by the \mathbf{s} to determine the non-zero coefficients. As shown in Fig. 6, our HeO outperforms both Lasso regression and the more advanced $L_{0.5}$ regression [40] in terms of producing more accurate indicators \mathbf{s} and achieving lower test prediction errors across various q and σ_ϵ settings. This reveals the efficiency of our HeO for mixed combinatorial optimization.

4.6 Constrained binary optimization

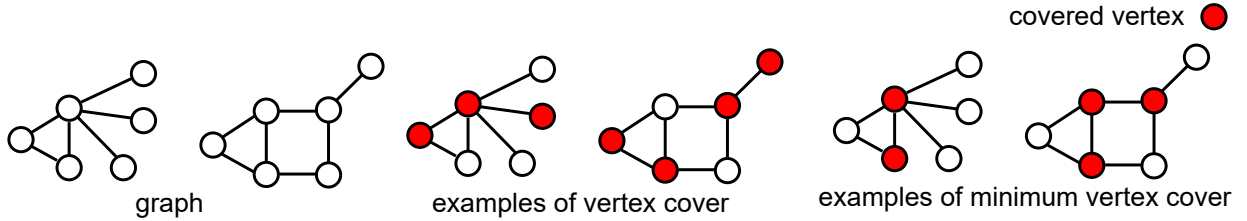


Figure 7: **The Heat diffusion optimization (HeO) framework.** The illustration of minimum vertex cover.

Table 1: The attributes of real world dataset and the vertex cover size of HeO and FastVC on them.

Graph name	Vertex number	Edge number	FastVC	HeO
tech-RL-caida	190914	607610	78306	77372.4 (17.4)
soc-youtube	495957	1936748	149458	148875.2 (25.0)
inf-roadNet-PA	1087562	1541514	588306	587401.0 (103.5)
inf-roadNet-CA	1957027	2760388	1063352	1061338.5 (31.9)
socfb-B-anon	2937612	20959854	338724	312531.4 (194.0)
socfb-A-anon	3097165	23667394	421123	387730.3 (355.3)
socfb-uci-uni	58790782	92208195	869457	867863.0 (36.3)

We now consider the combinatorial optimization problem involving multiple constraints, typically expressed as $g_k(\mathbf{s}) \leq 0$ for $k = 1, \dots, K$. One class of the constrained combinatorial optimization is minimum vertex cover (MVC), a constrained binary optimization problem with wide applications [43], as illustrated in Fig. 7. Given an undirected graph \mathcal{G} with vertex set \mathcal{V} and edge set \mathcal{E} , the MVC is to find the minimum subset $\mathcal{V}_c \subset \mathcal{V}$, so that for each edge $e \in \mathcal{E}$, at least one of its endpoints belongs to \mathcal{V}_c . The most popular approaches for tackling the MVC are heuristic algorithms [44].

We develop an algorithm leveraging HeO for tackling constrained MVC (Alg. 6, *Appendix*), where we transform these constraints into an unconstrained format by employing penalty coefficients λ . We compare the performance of HeO with the FastVC [44], a powerful MVC algorithm based on heuristic search on several real world graph datasets with massive vertex and edge number³. For a fair comparison, we control the run time of two algorithms as the same. As shown in Tab. 1e, our HeO identifies smaller cover sets in the same runtime as FastVC on massive real-world graphs. This

³<http://networkrepository.com/>

indicates the potential of our HeO for constrained binary optimization problems and highlights its low computational complexity.

5 Discussion

5.1 Related work

Several studies exhibit similarities to our HeO. Analogous to our HeO, the cross-entropy (CE) method [45] models the solution space of combinatorial optimization via a parameterized distribution, with iterative parameter updates. However, unlike HeO which requires only a single sample per iteration, the CE method updates parameters by increasing sample probabilities of improving the target function values, necessitating a large number of samples each iteration. Parallel to HeO, other methods integrate gradient information in combinatorial optimization. For example, the Gibbs-With-Gradient algorithm [46] employs gradients of the likelihood function relative to discrete inputs for more efficient exploration in the solution space. In contrast, our HeO explore the parameter space via gradient information from the target function. Sun et al. (2023) employ a denoising diffusion model (DDM) [24] for solving combinatorial optimization problems [47]. Though the DDM incorporates a diffusion process akin to the heat diffusion in our HeO, it diverges in key aspects, as discussed later. Moreover, akin to other deep learning-based solvers, this method necessitates a substantial dataset for training. In contrast, our HeO operates directly without training. Additionally, our HeO emerges as a variant of randomized smoothing, a technique applied to non-smooth convex optimization problems [48], known for its effectiveness in accelerating optimization procedure. A distinctive feature of our HeOs is that under different τ , the function $u(\tau, \theta)$ preserves the optima of the original target function $h(\theta)$. This unique property distinguishes the τ -diffusion (from $h(\theta)$ to $u(\tau, \theta)$) from the transformation in existing methods such as quantum adiabatic theory [9], bifurcation theory [12] and other relaxation strategies [49], in which there is inconsistency on the optima between the transformed and original one [27, 50]. This is also different from prior techniques that smooth the energy landscape by introducing noise while introducing bias to the optima simultaneously [51].

5.2 Relation to denoising diffusion models

Our approach, while bearing similarities to the DDM—a highly regarded and extensively utilized artificial generative model [24] that relies on the reverse diffusion process for data generation—differs in key aspects. The DDM necessitates reversing the diffusion process to generate data that aligns with the target distribution. In contrast, it is unnecessary for our HeO to strictly adhering to the reverse time sequence τ_t in the optimization process, as under different τ , the function $u(\tau, \theta)$ shares the same optima with that of the original problem $h(\theta)$. This claim is corroborated in Fig. S1, *Appendix*, where HeO applying nonmonotonic schedules of τ_t still demonstrates superior performance. Hence, it is possible to explore diverse τ_t schedules to further enhance the performance of the framework.

5.3 General parabolic differential equations

In this study, the heat diffusion equation forms the cornerstone of the proposed HeO. Broadly, HeO can be naturally extended to encompass general parabolic differential equations, given that a broad spectrum of these equations adhere to the property of backward uniqueness [52]. For example, we can apply a parabolic partial differential equation with constant coefficient to replace the Eq. (6):

$$\begin{cases} \partial_\tau u(\tau, \theta) = \nabla_\theta [A \nabla_\theta u(\tau, \theta)], & \tau > 0, \quad \theta \in \mathbb{R}^n \\ u(\tau, \theta) = h(\theta), & \tau = 0, \quad \theta \in \mathbb{R}^n \end{cases}, \quad (29)$$

where A is a real positive definite matrix. Our prior research demonstrated that the optimization of the denoising diffusion model can be significantly expedited by incorporating anisotropic Gaussian noise [53]. This implies that judiciously choosing a suitable matrix A could substantially improve the efficacy of the proposed framework in combinatorial optimization.

5.4 Limitations

Despite the effectiveness of HeO on the problems we have considered, it does have its limitations. Specifically, HeO demonstrates inefficiency in solving integer linear programming and routing problems, primarily due to the challenges in encoding integer variables through the probabilistic parameterization employed in our framework. However, integrating heat diffusion principles with advanced Metropolis-Hastings algorithm [54] presents a possible path to broaden the applicability of our concept to a wider range of combinatorial optimization problems.

6 Conclusion

In conclusion, grounded in the heat diffusion, we present a probabilistic parameterization framework called Heat diffusion optimization (HeO) to solve various combinatorial optimization problems. The heat diffusion facilitates the transmission of information from distant regions to the solver, thereby enhancing the efficiency in searching for the global optima. Demonstrating exceptional performance in numerous combinatorial optimization scenarios, our HeO underscores the potential of leveraging heat diffusion to overcome challenges associated with combinatorial explosion.

References

- [1] Francisco Barahona, Martin Grötschel, Michael Jünger, and Gerhard Reinelt. An application of combinatorial optimization to statistical physics and circuit layout design. *Operations Research*, 36(3):493–513, 1988.
- [2] Jun Wang, Tony Jebara, and Shih-Fu Chang. Semi-supervised learning using greedy max-cut. *The Journal of Machine Learning Research*, 14(1):771–800, 2013.
- [3] Chetan Arora, Subhashis Banerjee, Prem Kalra, and SN Maheshwari. An efficient graph cut algorithm for computer vision problems. In *Computer Vision—ECCV 2010: 11th European Conference on Computer Vision, Heraklion, Crete, Greece, September 5–11, 2010, Proceedings, Part III 11*, pages 552–565. Springer, 2010.
- [4] Hayato Ushijima-Mwesigwa, Christian FA Negre, and Susan M Mniszewski. Graph partitioning using quantum annealing on the d-wave system. In *Proceedings of the Second International Workshop on Post Moores Era Supercomputing*, pages 22–29, 2017.
- [5] Florian Neukart, Gabriele Compostella, Christian Seidel, David Von Dollen, Sheir Yarkoni, and Bob Parney. Traffic flow optimization using a quantum annealer. *Frontiers in ICT*, 4:29, 2017.
- [6] Román Orús, Samuel Mugel, and Enrique Lizaso. Quantum computing for finance: Overview and prospects. *Reviews in Physics*, 4:100028, 2019.
- [7] Rafael Marti and Gerhard Reinelt. *Exact and Heuristic Methods in Combinatorial Optimization*, volume 175. Springer, 2022.
- [8] Edward Farhi, Jeffrey Goldstone, Sam Gutmann, Joshua Lapan, Andrew Lundgren, and Daniel Preda. A quantum adiabatic evolution algorithm applied to random instances of an np-complete problem. *Science*, 292(5516):472–475, 2001.
- [9] John A Smolin and Graeme Smith. Classical signature of quantum annealing. *Frontiers in physics*, 2:52, 2014.
- [10] Joseph Bowles, Alexandre Dauphin, Patrick Huembeli, José Martinez, and Antonio Acín. Quadratic unconstrained binary optimization via quantum-inspired annealing. *Physical Review Applied*, 18(3):034016, 2022.
- [11] Mária Ercsey-Ravasz and Zoltán Toroczkai. Optimization hardness as transient chaos in an analog approach to constraint satisfaction. *Nature Physics*, 7(12):966–970, 2011.
- [12] Hayato Goto, Kosuke Tatsumura, and Alexander R Dixon. Combinatorial optimization by simulating adiabatic bifurcations in nonlinear hamiltonian systems. *Science advances*, 5(4):eaav2372, 2019.
- [13] Hayato Goto, Kotaro Endo, Masaru Suzuki, Yoshisato Sakai, Taro Kanao, Yohei Hamakawa, Ryo Hidaka, Masaya Yamasaki, and Kosuke Tatsumura. High-performance combinatorial optimization based on classical mechanics. *Science Advances*, 7(6):eabe7953, 2021.
- [14] Takahiro Inagaki, Yoshitaka Haribara, Koji Igarashi, Tomohiro Sonobe, Shuhei Tamate, Toshimori Honjo, Alireza Marandi, Peter L McMahon, Takeshi Umeki, Koji Enbutsu, et al. A coherent ising machine for 2000-node optimization problems. *Science*, 354(6312):603–606, 2016.
- [15] Egor S Tiunov, Alexander E Ulanov, and AI Lvovsky. Annealing by simulating the coherent ising machine. *Optics express*, 27(7):10288–10295, 2019.
- [16] Connor Bybee, Denis Kleyko, Dmitri E Nikonov, Amir Khosrowshahi, Bruno A Olshausen, and Friedrich T Sommer. Efficient optimization with higher-order ising machines. *Nature Communications*, 14(1):6033, 2023.
- [17] Martin JA Schuetz, J Kyle Brubaker, and Helmut G Katzgraber. Combinatorial optimization with physics-inspired graph neural networks. *Nature Machine Intelligence*, 4(4):367–377, 2022.
- [18] Bernardino Romera-Paredes, Mohammadamin Barekatain, Alexander Novikov, Matej Balog, M Pawan Kumar, Emilien Dupont, Francisco JR Ruiz, Jordan S Ellenberg, Pengming Wang, Omar Fawzi, et al. Mathematical discoveries from program search with large language models. *Nature*, pages 1–3, 2023.

- [19] David Pisinger and Stefan Ropke. Large neighborhood search. *Handbook of metaheuristics*, pages 99–127, 2019.
- [20] Pierre Hansen, Nenad Mladenović, and Jose A Moreno Perez. Variable neighbourhood search: methods and applications. *Annals of Operations Research*, 175:367–407, 2010.
- [21] Haoran Sun, Hanjun Dai, Wei Xia, and Arun Ramamurthy. Path auxiliary proposal for mcmc in discrete space. In *International Conference on Learning Representations*, 2021.
- [22] Lawrence C Evans. *Partial differential equations*, volume 19. American Mathematical Society, 2022.
- [23] Jean-Michel Ghidaglia. Some backward uniqueness results. *Nonlinear Analysis: Theory, Methods & Applications*, 10(8):777–790, 1986.
- [24] Ling Yang, Zhilong Zhang, Yang Song, Shenda Hong, Runsheng Xu, Yue Zhao, Wentao Zhang, Bin Cui, and Ming-Hsuan Yang. Diffusion models: A comprehensive survey of methods and applications. *ACM Computing Surveys*, 56(4):1–39, 2023.
- [25] Endre Boros and Peter L Hammer. Pseudo-boolean optimization. *Discrete applied mathematics*, 123(1-3):155–225, 2002.
- [26] Yves Crama and Peter L Hammer. *Boolean functions: Theory, algorithms, and applications*. Cambridge University Press, 2011.
- [27] Bernhard H Korte, Jens Vygen, B Korte, and J Vygen. *Combinatorial optimization*, volume 1. Springer, 2011.
- [28] Shakir Mohamed, Mihaela Rosca, Michael Figurnov, and Andriy Mnih. Monte carlo gradient estimation in machine learning. *The Journal of Machine Learning Research*, 21(1):5183–5244, 2020.
- [29] Avradip Mandal, Arnab Roy, Sarvagya Upadhyay, and Hayato Ushijima-Mwesigwa. Compressed quadratization of higher order binary optimization problems. In *Proceedings of the 17th ACM International Conference on Computing Frontiers*, pages 126–131, 2020.
- [30] Martin Anthony, Endre Boros, Yves Crama, and Aritanan Gruber. Quadratic reformulations of nonlinear binary optimization problems. *Mathematical Programming*, 162:115–144, 2017.
- [31] Michel Gendreau, Jean-Yves Potvin, et al. *Handbook of metaheuristics*, volume 2. Springer, 2010.
- [32] John J Hopfield and David W Tank. “neural” computation of decisions in optimization problems. *Biological cybernetics*, 52(3):141–152, 1985.
- [33] George Cybenko. Approximation by superpositions of a sigmoidal function. *Mathematics of control, signals and systems*, 2(4):303–314, 1989.
- [34] Zhe Wang, Alireza Marandi, Kai Wen, Robert L Byer, and Yoshihisa Yamamoto. Coherent ising machine based on degenerate optical parametric oscillators. *Physical Review A*, 88(6):063853, 2013.
- [35] Angelika Wiegele. Biq mac library—a collection of max-cut and quadratic 0-1 programming instances of medium size. *Preprint*, 51, 2007.
- [36] Holger H Hoos and Thomas Stützle. Satlib: An online resource for research on sat. *Sat*, 2000:283–292, 2000.
- [37] Andrew Lucas. Ising formulations of many np problems. *Frontiers in physics*, 2:5, 2014.
- [38] Amir Gholami, Sehoon Kim, Zhen Dong, Zhewei Yao, Michael W Mahoney, and Kurt Keutzer. A survey of quantization methods for efficient neural network inference. In *Low-Power Computer Vision*, pages 291–326. Chapman and Hall/CRC, 2022.
- [39] Robert Tibshirani. Regression shrinkage and selection via the lasso. *Journal of the Royal Statistical Society Series B: Statistical Methodology*, 58(1):267–288, 1996.
- [40] Zongben Xu, Hai Zhang, Yao Wang, XiangYu Chang, and Yong Liang. L 1/2 regularization. *Science China Information Sciences*, 53:1159–1169, 2010.
- [41] Trevor Hastie, Robert Tibshirani, Jerome H Friedman, and Jerome H Friedman. *The elements of statistical learning: data mining, inference, and prediction*, volume 2. Springer, 2009.
- [42] Xiaoping Li, Yadi Wang, and Rubén Ruiz. A survey on sparse learning models for feature selection. *IEEE transactions on cybernetics*, 52(3):1642–1660, 2020.
- [43] Alexander C Reis, Sean M Halper, Grace E Vezeau, Daniel P Cetnar, Ayaan Hossain, Phillip R Clauer, and Howard M Salis. Simultaneous repression of multiple bacterial genes using nonrepetitive extra-long sgrna arrays. *Nature biotechnology*, 37(11):1294–1301, 2019.
- [44] Shaowei Cai, Jinkun Lin, and Chuan Luo. Finding a small vertex cover in massive sparse graphs: Construct, local search, and preprocess. *Journal of Artificial Intelligence Research*, 59:463–494, 2017.

- [45] Pieter-Tjerk De Boer, Dirk P Kroese, Shie Mannor, and Reuven Y Rubinstein. A tutorial on the cross-entropy method. *Annals of operations research*, 134:19–67, 2005.
- [46] Will Grathwohl, Kevin Swersky, Milad Hashemi, David Duvenaud, and Chris Maddison. Oops i took a gradient: Scalable sampling for discrete distributions. In *International Conference on Machine Learning*, pages 3831–3841. PMLR, 2021.
- [47] Zhiqing Sun and Yiming Yang. Difusco: Graph-based diffusion solvers for combinatorial optimization. *Advances in neural information processing systems*, 2023.
- [48] John C Duchi, Peter L Bartlett, and Martin J Wainwright. Randomized smoothing for stochastic optimization. *SIAM Journal on Optimization*, 22(2):674–701, 2012.
- [49] Nikolaos Karalias and Andreas Loukas. Erdos goes neural: an unsupervised learning framework for combinatorial optimization on graphs. *Advances in Neural Information Processing Systems*, 33:6659–6672, 2020.
- [50] Haoyu Peter Wang, Nan Wu, Hang Yang, Cong Hao, and Pan Li. Unsupervised learning for combinatorial optimization with principled objective relaxation. *Advances in Neural Information Processing Systems*, 35:31444–31458, 2022.
- [51] Mo Zhou, Tianyi Liu, Yan Li, Dachao Lin, Enlu Zhou, and Tuo Zhao. Toward understanding the importance of noise in training neural networks. In *International Conference on Machine Learning*, pages 7594–7602. PMLR, 2019.
- [52] Jie Wu and Liqun Zhang. Backward uniqueness for general parabolic operators in the whole space. *Calculus of Variations and Partial Differential Equations*, 58:1–19, 2019.
- [53] Hengyuan Ma, Li Zhang, Xiatian Zhu, and Jianfeng Feng. Accelerating score-based generative models with preconditioned diffusion sampling. In *European Conference on Computer Vision*, pages 1–16. Springer, 2022.
- [54] Haoran Sun, Katayoon Goshvadi, Azade Nova, Dale Schuurmans, and Hanjun Dai. Revisiting sampling for combinatorial optimization. In *International Conference on Machine Learning*, pages 32859–32874. PMLR, 2023.
- [55] Juntao Wang, Daniel Ebler, KY Michael Wong, David Shui Wing Hui, and Jie Sun. Bifurcation behaviors shape how continuous physical dynamics solves discrete ising optimization. *Nature Communications*, 14(1):2510, 2023.

Appendix

1 Proof of theorems

To prove the Thm. 1, we recall the backward uniqueness of the heat equation [23].

Theorem S3. *Given two bounded function f_1, f_2 with domain on \mathbb{R}^n . Denote*

$$u_i(\tau, \mathbf{x}) = \mathbb{E}[f_i(\mathbf{x} + \sqrt{2\tau}\mathbf{z})] \quad (\text{S1})$$

for $i = 1, 2$, with $\mathbf{z} \sim \mathcal{N}(\mathbf{0}, I)$. If

$$u_1(\tau, \mathbf{x}) = u_2(\tau, \mathbf{x}), \quad \forall \mathbf{x} \in \mathbb{R}^n \quad (\text{S2})$$

for some $\tau > 0$, we have $f_1 = f_2$.

Proof of the Thm. 1.

Proof. We first show that the global maxima of $u(\tau, \boldsymbol{\theta})$ is also the global maxima of $h(\boldsymbol{\theta})$. The cornerstone of the proof is backward uniqueness of the heat equation [23], which asserts that the initial state of a heat equation can be uniquely determined by its state at a time point τ under mild conditions. To utilize the backward uniqueness, we consider the reparameterize $p(\mathbf{s}|\boldsymbol{\theta})$, so that $h(\boldsymbol{\theta})$ can be written as $\mathbb{E}_{p(\mathbf{x})}[f(\text{sgn}(\boldsymbol{\theta} - \mathbf{x}))]$ with $\mathbf{x} \sim \text{Unif}[0, 1]^n$. Using the definition of the heat kernel, we have

$$u(\tau, \boldsymbol{\theta}) = \mathbb{E}_{p(\mathbf{z})}[h(\boldsymbol{\theta} + \sqrt{2\tau}\mathbf{z})], \quad p(\mathbf{z}) = \mathcal{N}(\mathbf{0}, I). \quad (\text{S3})$$

Therefore, we have

$$u(\tau, \boldsymbol{\theta}) = \mathbb{E}_{p(\mathbf{z})}\mathbb{E}_{p(\mathbf{x})}[[f(\text{sgn}(\boldsymbol{\theta} + \sqrt{2\tau}\mathbf{z} - \mathbf{x}))]] = \mathbb{E}_{p(\mathbf{x})}[\mathbb{E}_{p(\mathbf{z})}[f(\text{sgn}(\boldsymbol{\theta} - (\mathbf{x} + \sqrt{2\tau}\mathbf{z})))]]. \quad (\text{S4})$$

Denote $u(\tau, \mathbf{x}; \boldsymbol{\theta}) = \mathbb{E}_{p(\mathbf{z})}[f(\text{sgn}(\boldsymbol{\theta} - (\mathbf{x} + \sqrt{2\tau}\mathbf{z})))]$, $\mathbf{x} \in (0, 1)^n$. Noticed that $u(\tau, \mathbf{x}; \boldsymbol{\theta})$ is the solution of the following unbounded heat diffusion equation restricted on $(0, 1)^n$

$$\begin{cases} \partial_\tau u(\tau, \mathbf{x}; \boldsymbol{\theta}) &= \Delta_{\mathbf{x}} u(\tau, \mathbf{x}; \boldsymbol{\theta}), & \tau > 0, & \mathbf{x} \in \mathbb{R}^n \\ u(\tau, \mathbf{x}; \boldsymbol{\theta}) &= f(\text{sgn}(\boldsymbol{\theta} - \mathbf{x})), & \tau = 0, & \mathbf{x} \in \mathbb{R}^n, \end{cases} \quad (\text{S5})$$

hence the latter can be considered as an extension of the former. Since $u(\tau, \mathbf{x}; \boldsymbol{\theta})$ is analytic respect to $\mathbf{x} \in (0, 1)^n$ for $\tau > 0$, this extension is unique. Therefore, the value of $u(\tau, \mathbf{x}; \boldsymbol{\theta})$ on $(0, 1)^n$, $\tau > 0$ uniquely determines the solution of Eq. (S5). Denote $\check{\boldsymbol{\theta}}$ as

$$\check{\theta}_i = \begin{cases} +\infty, & s_i^* = +1 \\ -\infty, & s_i^* = -1. \end{cases} \quad (\text{S6})$$

Then $u(\tau, \mathbf{x}; \check{\boldsymbol{\theta}}) = f^*$, for any $\tau \geq 0$ and $\mathbf{x} \in \mathbb{R}^n$, and we have

$$u(\tau, \check{\boldsymbol{\theta}}) = \mathbb{E}_{p(\mathbf{x})}[u(\tau, \mathbf{x}; \check{\boldsymbol{\theta}})] = f^*. \quad (\text{S7})$$

Noticed that

$$u(\tau, \boldsymbol{\theta}) = \mathbb{E}_{p(\mathbf{x})}[u(\tau, \mathbf{x}; \boldsymbol{\theta})] = \mathbb{E}_{p(\mathbf{x})}[\mathbb{E}_{p(\mathbf{z})}[f(\text{sgn}(\boldsymbol{\theta} - (\mathbf{x} + \sqrt{2\tau}\mathbf{z})))] \leq \mathbb{E}_{p(\mathbf{x})}[\mathbb{E}_{p(\mathbf{z})}[f^*]] = f^*, \quad \boldsymbol{\theta} \in \mathbb{R}^n. \quad (\text{S8})$$

where the equality is true if and only if $u(\tau, \mathbf{x}; \boldsymbol{\theta}) = f^*$ is true for $\mathbf{x} \in \mathbb{R}^n$. Therefore, if $\hat{\boldsymbol{\theta}}$ is the one of the maximas of $u(\tau, \boldsymbol{\theta})$, we have $u(\tau, \hat{\boldsymbol{\theta}}) = f^*$ and

$$u(\tau, \mathbf{x}; \hat{\boldsymbol{\theta}}) = f^* = u(\tau, \mathbf{x}; \boldsymbol{\theta}^*), \quad \mathbf{x} \in \mathbb{R}^n. \quad (\text{S9})$$

Due to the backward uniqueness of the heat diffusion equation, we have

$$u(0, \mathbf{x}; \hat{\boldsymbol{\theta}}) = u(0, \mathbf{x}; \boldsymbol{\theta}^*), \quad \mathbf{x} \in \mathbb{R}^n, \quad (\text{S10})$$

that is

$$h(\hat{\boldsymbol{\theta}}) = h(\boldsymbol{\theta}^*) = f^*. \quad (\text{S11})$$

As a result, $\hat{\boldsymbol{\theta}}$ is the one of maximas of $h(\boldsymbol{\theta})$. Conversely, using Eq. (S7), it is obviously to see that if $\hat{\boldsymbol{\theta}}$ is one of maximas of $h(\boldsymbol{\theta})$, it is also one of maximas of $u(\tau, \hat{\boldsymbol{\theta}})$. \square

Proof of the Thm. 2.

Proof. Define the square loss of θ as

$$e(\theta) = (h(\theta) - h(\theta^*))^2. \quad (\text{S12})$$

According to the definition of $h(\theta)$, we have

$$e(\theta) = \mathbb{E}_{p(\mathbf{x})}[f(\text{sgn}(\theta - \mathbf{x})) - f(\text{sgn}(\theta^* - \mathbf{x}))]^2 \leq \mathbb{E}_{p(\mathbf{x})}[(f(\text{sgn}(\theta - \mathbf{x})) - f(\text{sgn}(\theta^* - \mathbf{x})))^2]. \quad (\text{S13})$$

Define the error function

$$r(\tau, \mathbf{x}; \theta) = u(\tau, \mathbf{x}; \theta) - u(\tau, \mathbf{x}; \theta^*). \quad (\text{S14})$$

Then the error function satisfies the following heat equation

$$\begin{cases} \partial_\tau r(\tau, \mathbf{x}; \theta) = \nabla_{\mathbf{x}} r(\tau, \mathbf{x}; \theta) \\ r(0, \mathbf{x}; \theta) = f(\text{sgn}(\theta - \mathbf{x})) - f(\text{sgn}(\theta^* - \mathbf{x})). \end{cases} \quad (\text{S15})$$

Define the energy function of the error function $r(\tau, \mathbf{x}; \theta)$ as

$$E(\tau; \theta) = \int_{\mathbb{R}^n} r^2(\tau, \mathbf{x}; \theta) p(\mathbf{x}) d\mathbf{x}. \quad (\text{S16})$$

Then applying the heat equation and the integration by parts, we have

$$\frac{d}{d\tau} E(\tau; \theta) = -2 \int_{\mathbb{R}^n} \|\nabla r(\tau, \mathbf{x}; \theta)\|^2 p(\mathbf{x}) d\mathbf{x}. \quad (\text{S17})$$

Hence we have for $0 < \tau_1 < \tau_2$

$$E(\tau_1; \theta) = E(\tau_2; \theta) + 2 \int_{\tau_1}^{\tau_2} \int_{\mathbb{R}^n} \|\nabla r(\tau, \mathbf{x}; \theta)\|^2 p(\mathbf{x}) d\mathbf{x} d\tau. \quad (\text{S18})$$

Use the Harnack's inequality [22], we have

$$\|\nabla r(\tau, \mathbf{x}; \theta)\|^2 \leq r(\tau, \mathbf{x}; \theta) \partial_\tau r(\tau, \mathbf{x}; \theta) + \frac{n}{2\tau} r^2(\tau, \mathbf{x}; \theta), \quad (\text{S19})$$

hence, we have

$$E(\tau_1; \theta) \leq E(\tau_2; \theta) + \frac{n}{2} \int_{\tau_1}^{\tau_2} \frac{E(\tau; \theta)}{\tau} d\tau. \quad (\text{S20})$$

Using the Minkowski inequality on the measure $p(\mathbf{x})$, we have

$$\begin{aligned} e^{1/2}(\theta) &\leq \left(\int_{\mathbb{R}^n} (f(\text{sgn}(\theta - \mathbf{x})) - u(\tau_1; \mathbf{x}; \theta))^2 p(\mathbf{x}) d\mathbf{x} \right)^{1/2} + \left(\int_{\mathbb{R}^n} (u(\tau_1; \mathbf{x}; \theta) - u(\tau_1; \mathbf{x}; \theta^*))^2 p(\mathbf{x}) d\mathbf{x} \right)^{1/2} + \\ &\quad \left(\int_{\mathbb{R}^n} (f(\text{sgn}(\theta^* - \mathbf{x})) - u(\tau_1; \mathbf{x}; \theta^*))^2 p(\mathbf{x}) d\mathbf{x} \right)^{1/2} \\ &= \left(\int_{\mathbb{R}^n} (f(\text{sgn}(\theta - \mathbf{x})) - u(\tau_1; \mathbf{x}; \theta))^2 p(\mathbf{x}) d\mathbf{x} \right)^{1/2} + \left(\int_{\mathbb{R}^n} (f(\text{sgn}(\theta^* - \mathbf{x})) - u(\tau_1; \mathbf{x}; \theta^*))^2 p(\mathbf{x}) d\mathbf{x} \right)^{1/2} \\ &\quad + E^{1/2}(\tau_1; \theta). \end{aligned} \quad (\text{S21})$$

Recall the continuity of the heat equation:

$$\lim_{\tau \rightarrow 0} \int_{\mathbb{R}^n} (u(\tau, \mathbf{x}; \theta) - f(\text{sgn}(\theta - \mathbf{x})))^2 p(\mathbf{x}) d\mathbf{x} = 0. \quad (\text{S22})$$

Therefore, given $\epsilon > 0$, there exists a $\tau_1 > 0$, such that

$$\left(\int_{\mathbb{R}^n} (f(\text{sgn}(\theta - \mathbf{x})) - u(\tau_1; \mathbf{x}; \theta))^2 p(\mathbf{x}) d\mathbf{x} \right)^{1/2} + \left(\int_{\mathbb{R}^n} (f(\text{sgn}(\theta^* - \mathbf{x})) - u(\tau_1; \mathbf{x}; \theta^*))^2 p(\mathbf{x}) d\mathbf{x} \right)^{1/2} < \epsilon. \quad (\text{S23})$$

We then have the error control for $e(\theta)$:

$$e^{1/2}(\theta) \leq E^{1/2}(\tau_1; \theta) + \epsilon \leq (E(\tau_2; \theta) + \frac{n}{2} \int_{\tau_1}^{\tau_2} \frac{E(\tau; \theta)}{\tau} d\tau)^{1/2} + \epsilon. \quad (\text{S24})$$

Noticed that

$$E(\tau; \theta) \leq (f^* - f_{\min}) \mathbb{E}_{p(\mathbf{x})}[u(\tau, \mathbf{x}; \theta^*) - u(\tau, \mathbf{x}; \theta)] = (f^* - f_{\min})(u(\tau, \theta^*) - u(\tau, \theta)), \quad (\text{S25})$$

we prove the theorem. \square

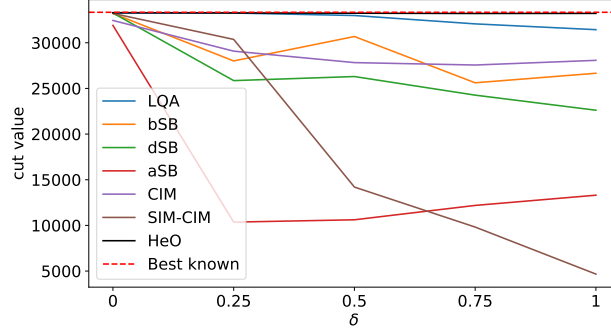


Figure S1: **Verifying the cooperative optimization mechanism of HeO.** The best cut value over 10 runs for each algorithm on the K-2000 problem [14] when the control parameters are randomly perturbed by different random perturbation level δ . The red dash line is the best cut value ever find.

2 Cooperative optimization

Our study suggests that HeO exhibits a distinct cooperative optimization mechanism, setting it apart from current methodologies. Specifically, HeO benefits from the fact that various τ -diffusion problems ($u(\tau, \theta)$) share the same optima as the original problem ($h(\theta)$). This characteristic allows the solver to transition between different τ values during the problem-solving process, eliminating the necessity for a monotonic τ_t schedule. In contrast, traditional methods such as those based on quantum adiabatic theory or bifurcation theory require a linear increase of a control parameter a_t from 0 to 1. This parameter is analogous to τ_t in the HeO framework.

To empirically verify the above claim, we introduce a random perturbation to the τ schedule in Alg. 1, rendering it non-monotonic: $\tilde{\tau}_t = c_t^2 \tau_t$, where c_t is uniformly distributed on $[1 - \delta, 1 + \delta]$ with δ controlling the amplitude of the perturbation. For other methods based on quantum adiabatic theory or bifurcation theory, we correspondingly introduce the perturbation as $\tilde{a}_t = \text{clamp}(c_t a_t, 0, 1)$. If an algorithm contains cooperative optimization mechanism, it still works well even when the control parameter is not monotonic, as optimizing the transformed problems under different control parameters cooperatively contributes to optimizing the original problem. As shown in S1, the performance of other methods are all dramatically deteriorated. In contrast, HeO shows no substantial decline in performance, corroborating that HeO employs a cooperative optimization mechanism.

3 Implementation details

Gradient descent with momentum. We provide HeO with momentum in Alg. 3.

Algorithm 3 Heat diffusion optimization (HeO) with momentum

Input: target function $f(\cdot)$, step size γ , momentum κ , τ schedule $\{\tau_t\}$, iteration number T
 initialize elements of θ_0 as 0.5
for $t = 0$ **to** $T - 1$ **do**
 sample $\mathbf{x}_t \sim \text{Unif}[0, 1]^n$
 $\mathbf{w}_t \leftarrow \nabla_{\theta_t} f(\text{erf}(\frac{\theta_t - \mathbf{x}_t}{\sqrt{2\tau_t}}))$
 $\mathbf{g}_t \leftarrow \kappa \mathbf{g}_{t-1} + \gamma \mathbf{w}_t$
 $\theta_{t+1} \leftarrow \text{Proj}_{\mathcal{I}}(\theta_t + \mathbf{g}_t)$
end for
 $\mathbf{s}_T \leftarrow \text{sgn}(\theta_T - 0.5)$
Output: binary configuration \mathbf{s}_T

Toy example. We set the momentum $\kappa = 0.9999$, learning rate $\gamma = 2$ and iteration number $T = 5000$, and $M = 1$ for HeO (Alg. 3). For MCGE, we set $T = 50000$, $\gamma = 1\text{e-}6$, momentum $\kappa = 0$, and $M = 10$. Empirically, we find that non-zero momentum results in worse results of MCGE.

Max-cut problem. For solving the max-cut problems from the Biq Mac Library [35], we set the steps $T = 5000$ for all the algorithms. For HeO, we set $\gamma = 2$, $M = 1$, and $\sqrt{2\tau_t}$ linearly decreases from 1 to 0 for HeO, and we set

momentum as zero. For LQA and SIM-CIM, we use the setting in [10]. For bSH, dSH, aSB, and CIM, we apply the settings in [55]. For each test, we estimate the mean and std from 10 runs.

3-SAT problem. For Boolean 3-satisfiability (3-SAT) problem, we set the momentum $\kappa = 0.9999$, $T = 5000$, $\gamma = 2$, $M = 1$, and $\sqrt{2\tau_t}$ linearly decreases from 1 to 0 for HeO. We consider the 3-SAT problems with various number of variables from the SATLIB [36]. For each number of variables in the dataset, we consider the first 100 instance. We apply the same configuration of that in [16] for both 3-order solver and 2-order oscillation Ising machine solver. The energy gap of the 2-order solver is set as 1. For each test, we estimate the mean and std from 100 runs.

Ternary-value neural network learning. We design the training algorithm for based on HeO in Alg. 4. The input \mathbf{v} of the dataset \mathcal{D} is generated from the uniform distribution on $\{-1, 0, 1\}^n$. For HeO, we set $T = 10000$, $\gamma = 0.5$, $\kappa = 0.999$, $M = 1$, and $\sqrt{2\tau_t}$ linearly decreasing from 1 to 0. For each test, we estimate the mean and std from 10 runs.

Algorithm 4 HeO for training ternary-value neural network.

Input: dataset \mathcal{D} , step size γ , momentum κ , τ schedule $\{\tau_t\}$, iteration number T
initialize elements of θ_0 as 1, initialize elements of $\tilde{\beta}_0$ as 0.
for $t = 0$ **to** $T - 1$ **do**
 sample $\mathbf{x}_t \sim \text{Unif}[0, 1]^n$
 $W_t \leftarrow W(\text{erf}(\frac{\theta_t - \mathbf{x}_t}{\sqrt{2\tau_t}}))$ (Eq. (26))
 $\text{MSE} \leftarrow \frac{1}{|\mathcal{D}|} \sum_{(\mathbf{v}, \mathbf{y}) \in \mathcal{D}} \|\Gamma(\mathbf{v}; W_t) - \mathbf{y}\|^2$
 $\mathbf{w}_t \leftarrow \nabla_{\theta_t} \text{MSE}$
 $\mathbf{g}_t \leftarrow \kappa \mathbf{g}_{t-1} + \gamma \mathbf{w}_t$
 $\theta_{t+1} \leftarrow \text{Proj}_{\mathcal{I}}(\theta_t - \mathbf{g}_t)$
end for
 $s_T = \text{sgn}(\theta_T - 0.5)$
Output: $W_T = W(s_T)$

Variable selection problem. We construct an algorithm for variable selection problem based on HeO as shown in Alg. 5, where the function $f(\mathbf{s}, \beta)$ is defined in Eq. (28).

Algorithm 5 HeO for linear regression variable selection

Input: dataset \mathcal{D} , step size γ , momentum κ , τ schedule $\{\tau_t\}$, iteration number T
initialize elements of θ_0 as 1, initialize elements of $\tilde{\beta}_0$ as 0.
for $t = 0$ **to** $T - 1$ **do**
 sample $\mathbf{x}_t \sim \text{Unif}[0, 1]^n$
 $\mathbf{w}_t^\theta \leftarrow \nabla_{\theta_t} f(\text{erf}(\frac{\theta_t - \mathbf{x}_t}{\sqrt{2\tau_t}}), \beta)$ (Eq. (28))
 $\mathbf{g}_t^\theta \leftarrow \kappa \mathbf{g}_{t-1}^\theta + \gamma \mathbf{w}_t^\theta$
 $\mathbf{w}_t^\beta \leftarrow \nabla_{\tilde{\beta}_t} f(\text{erf}(\frac{\theta_t - \mathbf{x}_t}{\sqrt{2\tau_t}}), \beta)$ (Eq. (28))
 $\mathbf{g}_t^\beta \leftarrow \kappa \mathbf{g}_{t-1}^\beta + \gamma \frac{\gamma}{T} \mathbf{w}_t^\beta$
 $\theta_{t+1} \leftarrow \text{Proj}_{\mathcal{I}}(\theta_t - \gamma \mathbf{g}_t^\theta)$
 $\tilde{\beta}_{t+1} \leftarrow \tilde{\beta}_t - \mathbf{g}_t^\beta$
end for
 $s_T \leftarrow \text{sgn}(\theta_T - 0.5)$
Output: s_T

We randomly generate 400-dimensional datasets with 1000 training samples. The element of the ground-truth coefficient β^* is uniformly distributed on $[-2, -1] \cup [1, 2]$, and each element has $1 - q$ probability of being set as zero and thus should be ignored for the prediction. We apply a five-fold cross-validation for all of methods. For our HeO, we set $T = 2000$ and $\gamma = 1$, $\kappa = 0.999$, and $M = 1$. We generate an ensemble of indicators \mathbf{s} of size 100. For each \mathbf{s} in the ensemble, we fit a linear model by implementing an OLS on the non-zero variables indicated by \mathbf{s} and calculate the average MSE loss of the linear model on the cross-validation sets. We then select the linear model with lowest MSE on the validate sets as the output linear model. For Lasso and $L_{0.5}$ regression, we follow the implementation in [40] with 10 iterations. the regularization parameter is selected by cross-validation from $\{0.05, 0.1, 0.2, 0.5, 1, 2, 5\}$. For each test, we estimate the mean and std from 10 runs.

Minimum vertex cover problem. For constrained binary optimization

$$\min_{\mathbf{s} \in \{1,1\}^n} f(\mathbf{s}), \quad (\text{S26})$$

$$g_k(\mathbf{s}) \leq 0, \quad k = 1, \dots, K, \quad (\text{S27})$$

we put the constrains as the penalty function with coefficient λ into the target function

$$f_\lambda(\mathbf{s}) = f(\mathbf{s}) - \lambda \sum_{k=1}^K g_k(\mathbf{s}), \quad (\text{S28})$$

propose the corresponding algorithm based on HeO, as shown in Alg. 6.

Algorithm 6 HeO for constrained binary optimization

Input: target function with penalty f_λ , step size γ , τ schedule $\{\tau_t\}$, penalty coefficients schedule $\{\lambda_t\}$, iteration number T
 initialize elements of θ_0 as 0.5
for $t = 0$ **to** $T - 1$ **do**
 sample \mathbf{x}_t from $\text{Unif}[0, 1]^n$
 $\mathbf{w}_t \leftarrow \nabla_{\theta_t} f_{\lambda_t}(\frac{\theta_t - \mathbf{x}_t}{\sqrt{2\tau}})$
 $\mathbf{g}_t \leftarrow \kappa \mathbf{g}_{t-1} + \gamma \mathbf{w}_t$
 $\theta_{t+1} \leftarrow \text{Proj}_{\mathcal{I}}(\theta_t - \gamma \mathbf{g}_t)$
end for
 $\mathbf{s}_T \leftarrow \text{sgn}(\theta_T - 0.5)$
Output: \mathbf{s}_T

Algorithm 7 Refinement of the result of MVC

Input: the result of HeO \mathbf{s}_T
for $i = 1$ **to** n **do**
 set $s_{T,i}$ as 0 if \mathbf{s}_T is still a vertex cover
end for
Output: \mathbf{s}_T

Table S2: The attributes of the real world graphs and the parameter settings of HeO.

graph name	$ V $	$ E $	T	γ	λ_t	σ_t
tech-RL-caida	190914	607610	200	2.5	linearly from 0 to 2.5	
soc-youtube	495957	1936748	200	2.5	linearly from 0 to 2.5	
inf-roadNet-PA	1087562	1541514	200	2.5	linearly from 0 to 7.5	
inf-roadNet-CA	1957027	2760388	200	5	linearly from 0 to 7.5	linearly from 1 to 0
socfb-B-anon	2937612	20959854	50	2.5	linearly from 0 to 5	
socfb-A-anon	3097165	23667394	50	2.5	linearly from 0 to 5	
socfb-uci-uni	58790782	92208195	50	2.5	linearly from 0 to 5	

We implement the HeO on a single NVIDIA RTX 3090 GPU for all the minimum vertex cover (MVC) experiments. Let \mathbf{s} be the configuration to be optimized, in which s_i is 1 if we select i -th vertex into \mathcal{V}_c , otherwise we do not select i -vertex into \mathcal{V}_c . The target function to be minimize is the size of \mathcal{V}_c : $f(\mathbf{s}) = \sum_{i=1}^n \frac{s_i+1}{2}$, and the constrains are

$$g_{ij}(\mathbf{s}) = (1 - \frac{s_i+1}{2})(1 - \frac{s_j+1}{2}) = 0, \quad \forall i, j, e_{ij} \in \mathcal{E}, \quad (\text{S29})$$

where e_{ij} represent the edge connecting the i and j -th vertices. We construct the target function $f_\lambda(\mathbf{s}) = f(\mathbf{s}) + \lambda \sum_{e_{ij} \in \mathcal{E}} g_{ij}(\mathbf{s})$. The term with the positive factor λ penalizes vector \mathbf{s} when there are uncovered edges. After the HeO outputs the result \mathbf{s}_T , we empirically find that its subset may also form a vertex cover for the graph \mathcal{G} , so we implement the following refinement on the result \mathbf{s}_T , as shown in Alg. 7. We report the vertex number, edge number and settings of HeO in Tab. S2. For FastVC, we follow the settings in [44] and use its codebase, and set the cut-off time as the same as the time cost of HeO. For each test, we estimate the mean and std from 10 runs.